

Evidence of phosphorus incorporation into InGaAs/InP epilayers after thermal annealing

S. Hernández, N. Blanco, I. Mártel, G. González-Daz, R. Cuscó, and L. Artús

Citation: [Journal of Applied Physics](#) **93**, 9019 (2003); doi: 10.1063/1.1565175

View online: <http://dx.doi.org/10.1063/1.1565175>

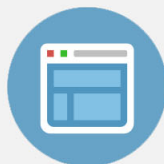
View Table of Contents: <http://scitation.aip.org/content/aip/journal/jap/93/11?ver=pdfcov>

Published by the [AIP Publishing](#)



Re-register for Table of Content Alerts

Create a profile.



Sign up today!



Evidence of phosphorus incorporation into InGaAs/InP epilayers after thermal annealing

S. Hernández

Institut Jaume Almera, Consell Superior d'Investigacions Científiques (CSIC), Lluís Solé i Sabarís s.n., 08028 Barcelona, Spain

N. Blanco, I. Mártil, and G. González-Díaz

Departamento de Física Aplicada III, Facultad de Física, Universidad Complutense, 28040 Madrid, Spain

R. Cuscó and L. Artús^{a)}

Institut Jaume Almera, Consell Superior d'Investigacions Científiques (CSIC), Lluís Solé i Sabarís s.n., 08028 Barcelona, Spain

(Received 16 May 2002; accepted 13 February 2003)

We report on Raman scattering measurements on annealed $\text{In}_{0.53}\text{Ga}_{0.47}\text{As}/\text{InP}$ layers that reveal the outdiffusion of phosphorus from the substrate and its possible incorporation in substitutional positions in the $\text{In}_{0.53}\text{Ga}_{0.47}\text{As}$ lattice. Raman signal associated with InP-like modes was detected in the annealed samples. The effect is also observed in samples where the substrate was protected by a $\text{SiN}_x:\text{H}$ capping and were annealed in arsenic atmosphere, thus ruling out the possibility of a surface contamination by atmospheric phosphorus evaporated from the InP substrate. Protruding regions of a few microns were observed on the surface, which were identified as misoriented $\text{In}_{1-x}\text{Ga}_x\text{P}$ and InP crystals by means of micro-Raman measurements. © 2003 American Institute of Physics. [DOI: 10.1063/1.1565175]

I. INTRODUCTION

Due to the higher electron mobility and velocity of $\text{In}_x\text{Ga}_{1-x}\text{As}$ relative to GaAs, and to the lower surface recombination velocity of the In-based materials, $\text{In}_x\text{Ga}_{1-x}\text{As}$ is an attractive material for applications in bipolar transistors, high-speed field-effect transistors, and microwave devices. $\text{In}_x\text{Ga}_{1-x}\text{As}$ is also a basic material for low dark-current, high-efficiency optoelectronic integrated circuits operating in the $1.55\text{ }\mu\text{m}$ range.¹ Developing a selective area doping technology is essential for single device and integrated circuit applications. At present, ion implantation is the only method for selectively introducing dopants in $\text{In}_x\text{Ga}_{1-x}\text{As}$ subsequent to growth, since no reliable diffusion technology exists for this material.² Because of the implantation-induced damage, a postimplantation annealing treatment is necessary to restore crystallinity and activate the dopants. It is well known that halogen lamp rapid thermal annealing (RTA) yields better electrical activation than conventional furnace annealing.³ In the particular case of Si^+ -implanted $\text{In}_x\text{Ga}_{1-x}\text{As}$, high values of electrical activation close to 100% have been reported for certain implantation/annealing conditions.^{3–6}

While it is generally assumed that the pure $\text{In}_x\text{Ga}_{1-x}\text{As}$ crystal is recovered after RTA, we have checked for possible alterations of the InGaAs/InP epilayers occurring during RTA under standard conditions for device processing. Such alterations may change the optical and electrical properties of the epilayers and consequently affect the quality of the devices produced by the implantation and annealing processes. It is well known that Raman scattering is a very powerful tech-

nique to assess crystal quality. Raman spectra are very sensitive to short- and long-range order in the crystal and, in particular, they provide valuable information about compositional alterations because such changes modify the vibrational properties of the crystal.

In this work, we investigate the effects of RTA on both unimplanted and Si^+ -implanted $\text{In}_{0.53}\text{Ga}_{0.47}\text{As}$ layers by means of Raman scattering and we show that the Raman spectra taken on the $\text{In}_{0.53}\text{Ga}_{0.47}\text{As}$ epilayers unambiguously reveal the presence of unexpected phosphorus in the region of the epilayer close to the surface. We have found similar results in samples where the InP substrate was covered by a $\text{SiN}_x:\text{H}$ protective capping to avoid possible phosphorus evaporation, which suggests that phosphorus diffusion from the substrate throughout the epilayer takes place during the annealing.

II. EXPERIMENT

The experiments were carried out on $\text{In}_{0.53}\text{Ga}_{0.47}\text{As}$ epilayers grown on (100) InP:Fe substrates by metalorganic vapor phase epitaxy, supplied by Epitaxial Products International Ltd. The samples were nominally undoped, with a donor concentration of $5 \times 10^{14}\text{ cm}^{-3}$ and an epilayer thickness of $1.9\text{ }\mu\text{m}$. 150 keV Si^+ ions were implanted at room temperature to a dose of $5 \times 10^{13}\text{ cm}^{-2}$ with the samples tilted 7° off the (100) direction to minimize channeling effects. Control samples were prepared with a $\text{SiN}_x:\text{H}$ protective capping covering the InP substrate to prevent P evaporation from the substrate. Both implanted and unimplanted samples were annealed at 905°C for 30 s in an MPT-600 reactor in an arsenic-rich ambient, using a graphite susceptor with the samples sandwiched between protective Si wafers in

^{a)}Electronic mail: lartus@ija.csic.es

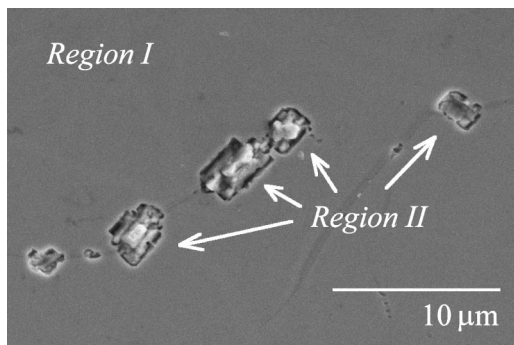


FIG. 1. Scanning electron micrograph of an $\text{In}_{0.53}\text{Ga}_{0.47}\text{As}$ epilayer after RTA at 905°C for 30 s showing defect-free areas (region I) and protruding lumps of crystalline material with dimensions of several microns (region II).

the so-called proximity geometry. To rule out the possibility of surface contamination with P, a set of annealed samples was wet etched in a $\text{H}_2\text{PO}_4:\text{H}_2\text{O}_2$ solution to remove a surface layer of about 400 nm. For the surface characterization by scanning electron microscopy (SEM), we have used a JEOL JSM 840 at 10 kV with a current of ≈ 100 pA. The annealed samples were analyzed by electroprobe x-ray microanalysis (EPXMA) in a CAMECA SX-50 microprobe, using a beam current of 100 nA and an electron energy of 5 keV, which probes to a depth $d \leq 300$ nm.

All of the Raman spectra presented in this work were obtained with a micro-Raman setup using the 514.5 nm line of an Ar^+ laser as an excitation source, with a power density of $\approx 5 \times 10^3$ W/cm² to minimize heating and photoexcitation effects. The scattered light was collected in backscattering geometry through a $\times 100$ objective and analyzed using a T64000 Jobin-Yvon spectrometer equipped with a liquid-nitrogen-cooled charge coupled device detector. The micro-Raman setup allowed a spatial resolution of about 1 μm .

III. RESULTS AND DISCUSSION

The examination under the optical microscope of the surface of the samples annealed at 905°C for 30 s revealed the presence of clusters of protruding material. Further analysis of the surface by means of SEM showed the existence of lumps of material with dimensions of a few microns that appear to develop over the surface in regions showing extended surface defects. Figure 1 shows a micrograph of the sample surface where two different regions can be distinguished: A flat defect-free region hereafter referred to as region I, and a set of defects corresponding to protruding material that we shall refer to as region II.

To investigate the annealing effects on the $\text{In}_{0.53}\text{Ga}_{0.47}\text{As}$ epilayer and to elucidate the origin of the defects induced by RTA, we have recorded Raman spectra of regions I and II. Figure 2 shows the $x(yz)\bar{x}$ Raman spectra obtained on region I of annealed $\text{In}_{0.53}\text{Ga}_{0.47}\text{As}$ epilayers, where x , y , and z denote $[100]$, $[010]$, and $[001]$ crystallographic directions of the substrate. The spectrum of the as-grown sample is included as a reference at the top of Fig. 2. In this spectrum, the GaAs-like longitudinal optical (LO) (269 cm^{-1}) and

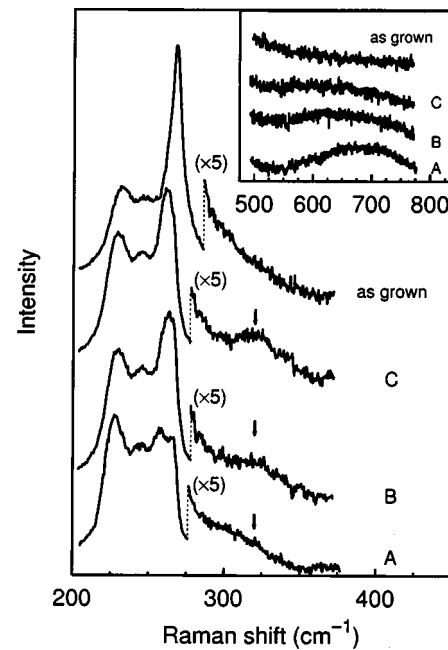


FIG. 2. $x(yz)\bar{x}$ Raman spectra of the annealed $\text{In}_{0.53}\text{Ga}_{0.47}\text{As}$ epilayers studied in this work compared with the spectrum of an as-grown $\text{In}_{0.53}\text{Ga}_{0.47}\text{As}$ sample (top). The figure shows the spectra of a Si^+ -implanted sample at 150 keV to $5 \times 10^{13}\text{ cm}^{-2}$ (curve A), an unimplanted sample after removal of a 400 nm surface layer by wet etching (curve B), and an unimplanted sample with a protective $\text{SiN}_x\text{:H}$ capping covering the InP substrate (curve C). The RTA treatments were carried out at 905°C for 30 s in an arsenic-rich atmosphere. The arrows indicate the location of the InP-like modes that can be observed in the annealed samples. The higher-frequency spectral range is shown in the inset, where a band due to the L_+ coupled modes can be seen in spectrum A.

InAs -like LO (232 cm^{-1}) peaks can be observed, as well as the disorder-related mode characteristic of $\text{In}_{0.53}\text{Ga}_{0.47}\text{As}$ at 242 cm^{-1} .^{7,8}

In Fig. 2(A), we show the Raman spectrum of the $\text{In}_{0.53}\text{Ga}_{0.47}\text{As}$ sample that was Si^+ implanted to $5 \times 10^{13}\text{ cm}^{-2}$ and subsequently annealed at 905°C for 30 s. For these implantation parameters, a peak electron density of $\approx 2 \times 10^{18}\text{ cm}^{-3}$ is generated⁶ and coupling of the free-electron plasma with the polar optical modes of the lattice takes place. As a consequence, the observed GaAs-like LO mode intensity is notably reduced, since it originates only in the surface depletion region, and features due to the three branches of the LO phonon-plasmon coupled modes show up in the spectrum. An additional peak at 257 cm^{-1} is detected between the disorder-related mode and the GaAs-like LO mode, which corresponds to the intermediate frequency coupled mode.⁹ The peak observed at 228 cm^{-1} , which displays a higher intensity than the InAs-like modes of the as-grown sample, can be assigned to the low-frequency coupled mode, which for high electron densities asymptotically approaches the InAs-like TO frequency.⁹ The plasmon-like L_+ coupled mode is smeared out by the inhomogeneous implantation profile, giving rise to a weak band between 550 and 800 cm^{-1} that can be clearly seen in curve A of the inset of Fig. 2. Besides the changes in the Raman spectrum associated with the plasmon-phonon coupled modes just discussed, an additional weak feature is observed around 325 cm^{-1} in

the spectrum of the implanted and annealed sample [Fig. 2(A)] that is not present in the spectrum of the as-grown $\text{In}_{0.53}\text{Ga}_{0.47}\text{As}$ sample. The frequency of this feature, found between the LO and transverse optical (TO) frequencies of InP, agrees well with the $\text{P:In}_{0.53}\text{Ga}_{0.47}\text{As}$ local mode frequency of $\approx 320\text{ cm}^{-1}$ estimated by extrapolating the Raman data reported for the $\text{In}_{1-x}\text{Ga}_x\text{As}_y\text{P}_{1-y}$ quaternary compound lattice matched to InP ($y/x \approx 2.2$), for low P composition.¹⁰ The $\text{In}_{1-x}\text{Ga}_x\text{As}_y\text{P}_{1-y}$ quaternary compound lattice matched to InP was reported to exhibit a pseudo-two-mode behavior, with two well separated optical bands associated with arsenic and phosphorus vibrations.¹⁰ Later studies^{11,12} have suggested a four-mode behavior, where GaAs-, InAs-, InP-, and GaP-like modes can be resolved. With increasing P composition, the InP-like LO frequency increases from an extrapolated $\text{P:In}_{0.53}\text{Ga}_{0.47}\text{As}$ local mode frequency of $\approx 320\text{ cm}^{-1}$ up to the InP LO frequency, whereas the GaAs-like LO frequency decreases from the GaAs-like LO frequency of $\text{In}_{0.53}\text{Ga}_{0.47}\text{As}$ (269 cm^{-1}) to an extrapolated frequency of about 240 cm^{-1} for vanishing Ga concentration.¹⁰ Thus, the incorporation of P into the $\text{In}_{1-x}\text{Ga}_x\text{As}$ lattice results in a downward shift of the $\text{In}_{1-x}\text{Ga}_x\text{As}$ modes. Such a shift is indeed observed in the spectrum of Fig. 2(A), where the GaAs-like LO mode is found about 5 cm^{-1} below the GaAs-like LO mode frequency of the as-grown $\text{In}_{0.53}\text{Ga}_{0.47}\text{As}$. The small frequency shift of the InGaAs-like LO modes and the low intensity of the InP-like modes suggest that the P composition of the quaternary alloy is quite small.¹⁰

In Figs. 2(B) and 2(C), we show the Raman spectra obtained from annealed unimplanted $\text{In}_{0.53}\text{Ga}_{0.47}\text{As}$ samples, where both the InP-like LO mode (indicated by the arrows) and the downward frequency shift of the GaAs-like LO mode can be clearly seen. Therefore, the P incorporation into the $\text{In}_{0.53}\text{Ga}_{0.47}\text{As}$ lattice appears to be associated with the annealing step. Since the optical absorption in $\text{In}_x\text{Ga}_{1-x}\text{As}$ is very high for the 514.5 nm wavelength, $\alpha = 2.23 \times 10^5\text{ cm}^{-1}$,¹³ the Raman scattering probing depth is quite small, $z = 1/2\alpha = 2.24 \times 10^{-6}\text{ cm}$, and only a region close to the surface is probed in the experiments. This rules out the possibility of observing the LO InP mode from the substrate, which, on the other hand, occur at higher frequencies than the InP-like LO modes observed in Fig. 2. Contrary, the possibility that the observed InP-like modes arise from a shallow surface contamination of the sample with phosphorus should be considered. To rule out this possibility, a 400 nm surface layer was removed by wet etching to ensure that a deeper region of the epilayer was probed by the Raman measurements. The Raman spectrum obtained from the annealed and etched sample is shown in Fig. 2(B). The distinctive features that indicate the quaternary alloy formation, namely the presence of the InP-like peak at $\approx 325\text{ cm}^{-1}$ and the shift to lower frequencies of the InGaAs-like modes, remain clearly observed. These results show that P incorporation occurs throughout the $\text{In}_{1-x}\text{Ga}_x\text{As}$ epilayer during the annealing, independently from previous implantation processes, and suggest P outdiffusion from the InP substrate as the source of phosphorus. Although the typical diffusivity of P in defect-free GaAs crystals is far too low to explain the presence of P

throughout the $\text{In}_{1-x}\text{Ga}_x\text{As}$ epilayer, pipe diffusion along dislocations can greatly increase the penetration depth of P leading to diffusion coefficients several orders of magnitude higher than the diffusion coefficient in a defect-free crystal.^{13,14} The presence of a relatively high dislocation density in the $\text{In}_{1-x}\text{Ga}_x\text{As}$ epilayers may have favored the P incorporation throughout the whole epilayer thickness. Also, phosphorus diffusion may have been greatly enhanced by the presence of group-V vacancies created due to arsenic desorption at the surface during the annealing process, which quickly diffuse into the epilayer.

To confirm that the observed P is diffusing from the substrate, an $\text{In}_{0.53}\text{Ga}_{0.47}\text{As}$ sample was prepared prior to annealing with a protective $\text{SiN}_x\text{:H}$ capping layer covering the InP substrate, so as to prevent P evaporation from the substrate to the annealing atmosphere and to enhance the P diffusion through the epilayer. In Fig. 2(C), we display the Raman spectrum obtained from this sample after RTA under the same conditions, where the characteristic features of the $\text{In}_{1-x}\text{Ga}_x\text{As}_y\text{P}_{1-y}$ quaternary alloy already discussed can be observed even more clearly. Both the intensity of the InP-like modes and the downward shift of the GaAs-like modes in the capped sample are slightly higher than in the etched sample, indicating a slightly higher P composition of the alloy in the capped sample. We performed EPXMA measurements on samples B and C that confirmed the presence of phosphorus in the $\text{In}_{1-x}\text{Ga}_x\text{As}$ epilayer. The P atom concentration was consistently found to be of a few percent, slightly higher in the capped sample. The higher P concentration obtained for the capped sample was to be expected, given the constraint imposed by the capping layer that forces the phosphorus to diffuse through the $\text{In}_{1-x}\text{Ga}_x\text{As}$ epilayer during the annealing.

Next, we focus on the protruding lumps of material observed in the annealed samples (region II). Typical Raman spectra obtained from various lumps are shown in Figs. 3(A) and 3(B). These spectra exhibit marked differences in relation to the spectra of region I displayed in Fig. 2. The most striking feature of the spectra of region II is the presence of two intense broad peaks in the $300\text{--}380\text{ cm}^{-1}$ range, in contrast with the very weak InP-like modes detected in this frequency range in the Raman spectra of region I. The high intensity of these modes indicates a significantly higher P concentration in region II. Moreover, the high-frequency peak is located above the InP LO frequency, which can only be explained by the presence of Ga in the alloy that is formed in region II. In fact, the frequencies of the observed peaks are in good agreement with reported data on TO and LO modes of the $\text{In}_{1-x}\text{Ga}_x\text{P}$ ternary alloy.^{15,16} The frequency of these peaks shows variations from spot to spot, as can be seen from the spectra of Figs. 3(A) and 3(B), indicating that the Ga concentration varies over the different spots of region II. From the observed $\text{In}_{1-x}\text{Ga}_x\text{P}$ mode frequencies and the reported frequency dependence of the optical $\text{In}_{1-x}\text{Ga}_x\text{P}$ modes,¹⁵ the Ga concentration in the spots of region II can be roughly estimated, and it is found to be around 25% for spectrum (A) and 18% for spectrum (B). Given that Raman scattering by TO modes is forbidden in backscattering from a (100) face, the observation of intense TO modes in the spec-

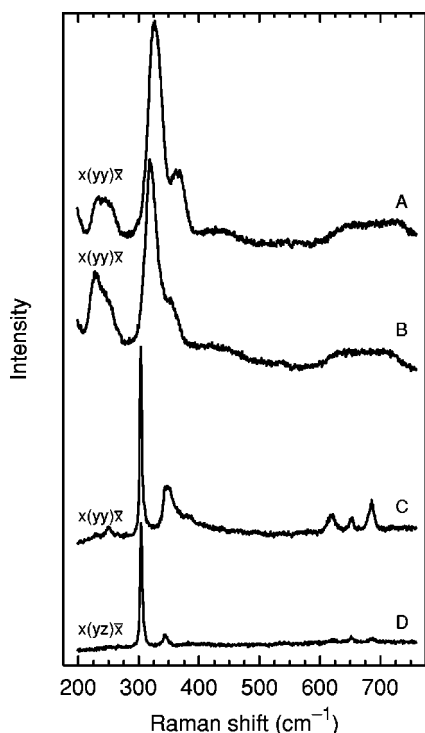


FIG. 3. Raman spectra of the protruding material observed in $\text{In}_{0.53}\text{Ga}_{0.47}\text{As}$ epilayers after RTA: A typical parallel-polarization spectrum (curve A); same for an implanted and annealed sample (curve B), parallel-polarization spectrum on a lump that shows the existence of pure InP crystals (curve C), and crossed-polarization spectrum of the same spot (curve D). The polarization directions are referred to the substrate crystallographic axes.

tra indicates the crystal misorientation in region II. While the lattice mismatch and misorientation of the material may be partly accommodated by the presence of dislocations and defects around these spots, a high degree of disorder is present in the alloy as indicated by the broad $\text{In}_{1-x}\text{Ga}_x\text{P}$ optical mode peaks.

Three weaker structures are also observed in the spectra of Figs. 3(A) and 3(B). First, a flat band in the 600–750 cm^{-1} range, which extends from twice the $\text{In}_{1-x}\text{Ga}_x\text{P}$ TO frequency up to twice the $\text{In}_{1-x}\text{Ga}_x\text{P}$ LO frequency, can be readily associated with the second-order optical modes of $\text{In}_{1-x}\text{Ga}_x\text{P}$.¹⁶ No individual second-order peaks can be resolved, which confirms the high degree of disorder present in the alloy. Second, a featureless band in the InGaAs-like optical mode region, which can be ascribed to a residual presence of As in region II material. The low intensity of this band as compared with the InGaAs-like modes observed in Fig. 2 indicates that the As concentration is very small. In contrast with region I, and on account of the low As concentration and the high degree of disorder in the alloy, no distinct peaks associated with GaAs-like or InAs-like modes can be resolved. Third, a weak feature can be observed centered at about 430 cm^{-1} . A similar structure was observed in heavily implanted InP^{17,18} and assigned to P–P vibrations in phosphorus clusters.¹⁹ The detection of P–P vibrations associated with phosphorus clusters provides further evidence that a substantial phosphorus diffusion occurs through region II areas and it shows that not all the diffused P atoms are

substitutionally incorporated to the crystal lattice in these areas.

Some spots of region II exhibit very high In concentrations and very low As content. This is dramatically evidenced by the Raman spectra of pure, well-crystallized InP obtained from one of such spots, which are displayed in Figs. 3(C) and 3(D). In fact, an intense sharp peak is observed at 303 cm^{-1} corresponding to the InP TO mode.²⁰ The very good crystallinity of the InP material is confirmed by the observation of the characteristic three second-order optical-mode peaks of InP,²⁰ which are clearly detected between 600 and 700 cm^{-1} . The InP LO mode is detected as a very weak peak at 343 cm^{-1} in crossed polarizations [Fig. 3(D)], whereas the parallel polarization spectrum [Fig. 3(C)] exhibits a more intense broader peak centered at 348 cm^{-1} that corresponds to the photoexcited L_+ phonon-plasmon coupled modes.²¹ Thus, according to the Raman spectra shown in Figs. 3(C) and 3(D), the LO mode and the L_+ coupled mode are allowed in parallel polarization and forbidden in crossed polarization configuration, whereas the TO modes are allowed in both polarization configurations. So, Raman scattering from these spots appears to follow the selection rules for backscattering from a (111) face rather than from a (100) face.

The Raman scattering results presented herein clearly show the incorporation of phosphorus to the $\text{In}_x\text{Ga}_{1-x}\text{As}$ lattice. Even though only mixed-crystal modes associated with substitutional P in anion positions are detected by means of Raman scattering, a fraction of the diffused phosphorus may well be incorporated in cation positions. Considering that P substitutes for As in the annealed $\text{In}_{0.53}\text{Ga}_{0.47}\text{As}$ epilayers, as shown by the Raman spectra reported in this work, the incorporation of P in Ga positions seems likely given the similar covalent radius and mass of Ga and As. Phosphorus impurities in antisite positions of the $\text{In}_x\text{Ga}_{1-x}\text{As}$ crystal act as double donors and, therefore, the phosphorus diffusion may contribute to increase the free-electron density in the annealed samples, which could explain the anomalous high electrical activations observed in implanted and annealed $\text{In}_{0.53}\text{Ga}_{0.47}\text{As}$ samples.^{3–6} In fact, this effect may be even more important in implanted samples where a significant fraction of the group-III atoms have been displaced by the ion beam bombardment and P may tend to occupy Ga sites upon annealing.

IV. CONCLUSIONS

We have shown that a phosphorus incorporation into $\text{In}_{0.53}\text{Ga}_{0.47}\text{As}$ epilayers takes place during RTA carried out under standard annealing conditions that are commonly used in device processing, resulting in the formation of an $\text{In}_{1-x}\text{Ga}_x\text{As}_y\text{P}_{1-y}$ alloy. Although our results indicate that phosphorus preferentially accumulates along extended defects, leading to the formation of misoriented $\text{In}_{1-x}\text{Ga}_x\text{P}$ crystalline lumps visible on the surface, the micro-Raman measurements presented in this work show that phosphorus incorporation occurs over the whole $\text{In}_{0.53}\text{Ga}_{0.47}\text{As}$ epilayer. This is evidenced by the observation of weak InP-like modes in the flat region of the epilayer, which indicate a consis-

tently low P composition of the $\text{In}_{1-x}\text{Ga}_x\text{As}_y\text{P}_{1-y}$ alloy formed in the epilayer. By contrast, the Ga concentration in the protruding $\text{In}_{1-x}\text{Ga}_x\text{P}$ regions exhibits sizable variations. Although typical Ga concentrations are around 20%, even pure InP crystals have been identified in these regions.

After ruling out other possible sources for the phosphorus incorporation, we conclude that the observed phosphorus must come from the InP substrate, probably enhanced by pipe diffusion along dislocations. The possible incorporation of a small fraction of the diffused P atoms in antisite positions, acting as donor impurities, may contribute to the high electrical activation measured in some of the Si^+ -implanted samples.

ACKNOWLEDGMENTS

The authors wish to thank Professor J. Jiménez for his useful comments on the manuscript. This work was partially supported by DGICYT Grant No. PB97-1254 and by CICYT Grant No. TIC-98/0740. One of the authors (S. H.) acknowledges support from Departament d'Universitats i Recerca de la Generalitat de Catalunya.

¹F. E. Ejeckam, C. L. Chua, Z. H. Zhu, Y. H. Lo, M. Hong, and R. Bhat, *Appl. Phys. Lett.* **67**, 3936 (1995).

²M. V. Rao, *Nucl. Instrum. Methods Phys. Res. B* **79**, 645 (1993).

³M. V. Rao, S. M. Gulwadi, P. E. Thompson, A. Fathimulla, and O. A. Aina, *J. Electron. Mater.* **18**, 131 (1989).

⁴T. Penna, B. Tell, A. S. H. Liao, T. J. Bridges, and G. Burkhardt, *J. Appl. Phys.* **57**, 351 (1985).

⁵M. V. Rao and W. Kruppa, *Electron. Lett.* **22**, 299 (1986).

⁶M. N. Blanco, E. Redondo, F. Calle, I. Mártel, and G. González-Díaz, *J. Appl. Phys.* **87**, 3478 (2000).

⁷T. P. Pearsall, R. Carles, and J. C. Portal, *Appl. Phys. Lett.* **42**, 436 (1983).

⁸J. P. Estrera, P. D. Stevens, R. Glosser, W. M. Duncan, Y. C. Kao, H. Y. Liu, and E. A. Beam III, *Appl. Phys. Lett.* **61**, 1927 (1992).

⁹R. Cuscó, L. Artús, S. Hernández, J. Ibáñez, and M. Hopkinson, *Phys. Rev. B* **65**, 035210 (2002).

¹⁰A. Pinczuk, J. M. Worlock, R. E. Nahory, and M. A. Pollack, *Appl. Phys. Lett.* **33**, 461 (1978).

¹¹R. K. Soni, S. C. Abbi, K. P. Jain, M. Balkanski, S. Slempek, and J. L. Benchimol, *J. Appl. Phys.* **59**, 2184 (1986).

¹²B. Jusserand and S. Slempek, *Solid State Commun.* **49**, 95 (1984).

¹³S. M. Kelso, D. E. Aspnes, M. A. Pollack, and R. E. Nahory, *Phys. Rev. B* **26**, 6669 (1982).

¹⁴R. F. Scholz and U. Gösele, *J. Appl. Phys.* **87**, 704 (2000).

¹⁵R. Beserman, C. Hirlimann, M. Balkanski, and J. Chevalier, *Solid State Commun.* **20**, 485 (1976).

¹⁶E. Bedel, R. Carles, G. Landa, and J. B. Renucci, *Rev. Phys. Appl.* **19**, 17 (1984).

¹⁷S. J. Yu, H. Asahi, S. Emura, H. Sumida, S. Gonda, and H. Tanoue, *J. Appl. Phys.* **66**, 856 (1989).

¹⁸R. Cuscó, G. Talamás, L. Artús, J. M. Martín, and G. González-Díaz, *J. Appl. Phys.* **79**, 3927 (1996).

¹⁹M. Wühl, M. Cardona, and J. Tauc, *J. Non-Cryst. Solids* **8**, 172 (1972).

²⁰L. Artús, R. Cuscó, J. Ibáñez, J. M. Martín, and G. González-Díaz, *J. Appl. Phys.* **82**, 3736 (1997).

²¹R. Cuscó, J. Ibáñez, and L. Artús, *Phys. Rev. B* **57**, 12 197 (1998).